

Reduced Hepatic Uptake and Intestinal Excretion of Organic Cations in Mice with a Targeted Disruption of the Organic Cation Transporter 1 (*Oct1* [*Slc22a1*]) Gene

JOHAN W. JONKER,¹ ELS WAGENAAR,¹ CARLA A. A. M. MOL,² MARIJE BUITELAAR,¹
HERMANN KOEPEL,³ JOHAN W. SMIT,¹ AND ALFRED H. SCHINKEL^{1*}

*Division of Experimental Therapy¹ and Division of Molecular Biology², The Netherlands Cancer Institute,
1066 CX Amsterdam, The Netherlands, and Anatomisches Institut, Bayerische
Julius-Maximilians-Universität, 97070 Würzburg, Germany³*

Received 7 February 2001/Returned for modification 16 April 2001/Accepted 23 May 2001

The polyspecific organic cation transporter 1 (OCT1 [SLC22A1]) mediates facilitated transport of small (hydrophilic) organic cations. OCT1 is localized at the basolateral membrane of epithelial cells in the liver, kidney, and intestine and could therefore be involved in the elimination of endogenous amines and xenobiotics via these organs. To investigate the pharmacologic and physiologic role of this transport protein, we generated *Oct1* knockout (*Oct1*^{−/−}) mice. *Oct1*^{−/−} mice appeared to be viable, healthy, and fertile and displayed no obvious phenotypic abnormalities. The role of Oct1 in the pharmacology of substrate drugs was studied by comparing the distribution and excretion of the model substrate tetraethylammonium (TEA) after intravenous administration to wild-type and *Oct1*^{−/−} mice. In *Oct1*^{−/−} mice, accumulation of TEA in liver was four to sixfold lower than in wild-type mice, whereas direct intestinal excretion of TEA was reduced about twofold. Excretion of TEA into urine over 1 h was 53% of the dose in wild-type mice, compared to 80% in knockout mice, probably because in *Oct1*^{−/−} mice less TEA accumulates in the liver and thus more is available for rapid excretion by the kidney. In addition, we found that absence of Oct1 leads to decreased liver accumulation of the anticancer drug metaiodobenzylguanidine and the neurotoxin 1-methyl-4-phenylpyridinium. In conclusion, our data show that Oct1 plays an important role in the uptake of organic cations into the liver and in their direct excretion into the lumen of the small intestine.

The facilitated transport of organic cations, which include many clinically used drugs and endogenous compounds, is mediated by the family of organic cation transport proteins (OCT [SLC22A]). This family currently consists of five members: OCT1, OCT2, and OCT3 (6, 7, 21, 23, 33) and the more distantly related OCTN1 (26) and OCTN2 (34). The organic cation transporters are localized in the plasma membrane of epithelial cells and are characterized by a predicted 12-transmembrane-domain (TMD) structure and a large extracellular hydrophilic loop between TMD1 and TMD2 (reviewed in references 4 and 13). In rodents, *Oct1* (*Slc22a1*) is highly expressed in the liver, kidney, and small intestine (7, 23), whereas in humans it is expressed primarily in the liver (6). In vitro, Oct1 mediates the facilitated diffusion of small, relatively hydrophilic cations, including the model compounds tetraethylammonium (TEA) and *N*¹-methylnicotinamide, the neurotoxin 1-methyl-4-phenylpyridinium (MPP⁺), and also monoamine transmitters such as adrenaline and dopamine (1, 35). Larger, more hydrophobic cations like the antiarrhythmics quinine and quinidine are inhibitors of Oct1-mediated transport but are not transported by Oct1 (18). Oct2 has a substrate specificity similar to that of Oct1, but its expression is limited to the kidney and specific regions in the brain (8). The distribution of Oct1 and Oct2 in tissues has been studied by immunohistochemistry

in the rat. Oct1 is localized at the sinusoidal (basolateral) membrane of hepatocytes in the liver, whereas in the kidney both Oct1 and Oct2 are localized at the basolateral membrane of epithelial cells lining the proximal tubules (12, 16, 29). This strategic localization of Oct1 and Oct2 in excretory organs suggests that they play a crucial role in the elimination of cationic drugs and other compounds from the body by mediating entry of these compounds from the blood into the excretory epithelial cells. Due to the absence of good in vivo models, however, the exact biological functions of Oct1 and Oct2 are still not well understood.

To study these functions, we generated a knockout mouse line that lacks functional Oct1. *Oct1*^{−/−} mice are healthy and fertile but display an impaired liver uptake and direct intestinal excretion of substrate organic cations, indicating that Oct1 plays an essential role in the disposition of organic cations to liver and intestine.

MATERIALS AND METHODS

Animals. Mice were housed and handled according to institutional guidelines complying with Dutch legislation. Unless stated otherwise, the animals used in all experiments were *Oct1*^{−/−} or wild-type mice, of comparable mixed genetic background (on average 50% 129/OLA and 50% FVB), between 9 and 14 weeks of age. Animals were kept in a temperature-controlled environment with a 12-h light/12-h dark cycle. They received a standard diet (AM-II; Hope Farms, Woerden, The Netherlands) and acidified water ad libitum.

Materials. [¹⁴C]TEA (55 Ci/mol) was from American Radiolabeled Chemicals, Inc. (St. Louis, Mo.); [³H]MPP⁺ (82 Ci/mmol) and [¹⁴C]choline (54 Ci/mol) were from NEN Life Science Products, Inc. (Boston, Mass.); [³H]cimetidine (15.5 Ci/mmol) was from Amersham Life Science (Little Chalfont, United Kingdom); MPP⁺ iodide was from Research Biochemicals International (Natick,

* Corresponding author. Mailing address: Division of Experimental Therapy, The Netherlands Cancer Institute, Plesmanlaan 121, 1066 CX Amsterdam, The Netherlands. Phone: 31-20-5122046. Fax: 31-20-5122050. E-mail: alfred@nki.nl.

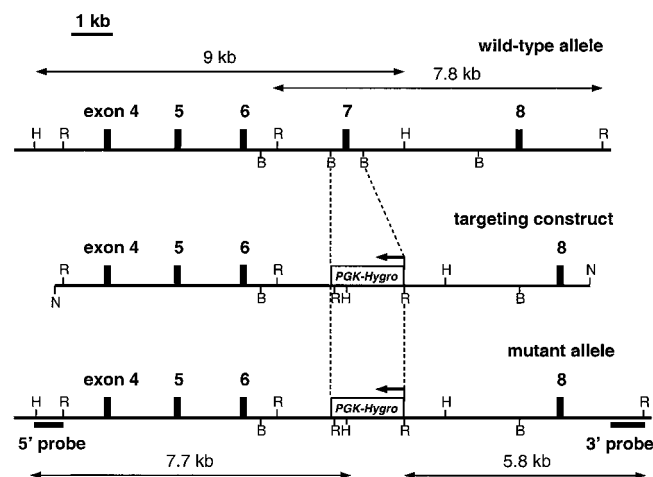


FIG. 1. Targeted disruption of the *Oct1* gene by homologous recombination. In structures of the wild-type and mutant alleles and the targeting construct, exons are indicated by closed boxes (exact positions and sizes of exons are not drawn to scale). In the targeting construct, exon 7 was replaced with an inverted (as indicated with an arrow) *pgk-hygro* cassette. Only relevant restriction sites are indicated: H, *HindII*; R, *EcoRV*; B, *BamHI*; N, *NotI*. For Southern analysis, 5' and 3' probes were used on *HindII* (5') and *EcoRV* (3') digested genomic DNA. Sizes of diagnostic restriction fragments for wild-type and targeted alleles are indicated by double-headed arrows (drawn to scale).

Mass.); ketamine (Ketalar) was from Parke-Davis (Hoofddorp, The Netherlands); choline [(2-hydroxyethyl)trimethylammonium chloride] and xylazine were from Sigma Chemical Co. (St. Louis, Mo.); methoxyflurane (Metofane) was from Medical Developments Australia Pty. Ltd. (Springvale, Victoria, Australia); 125 I-labeled metaiodobenzylguanidine (MIBG; 7 Ci/mmol) was synthesized as described elsewhere (32); anti-rat cytochrome P450 3A1 (monoclonal) was from Oxford Biomedical Research, Inc. (Oxford, Mich.); donkey anti-rabbit immunoglobulin (Ig), F(ab')₂ fragment, was from Amersham Pharmacia Biotech; goat anti-mouse Ig was from DAKO (Glostrup, Denmark); TEA was from Fluka Chemie AG (Buchs, Switzerland). All other compounds were reagent grade.

Cloning of 129/OLA *Oct1* genomic DNA and construction of the targeting vector. Mouse *Oct1* genomic DNA sequences were cloned from a 129/OLA-derived genomic library constructed in bacteriophage λ GEM12. By screening with *Oct1*-specific cDNA probes, a genomic sequence containing exons 4 to 8 homologous to human *OCT1* was identified and cloned into the pGEM5 vector (Promega), using *NotI* digestion. From this construct, a 5-kb *BglII* fragment was subcloned into the pSP72 vector (Promega). By partial digestion with *BamHI*, a 0.8-kb fragment containing exon 7 was deleted from this construct and replaced with a 1.8-kb *BglII*-*BglII* *pgk-hygro* cassette in reverse transcriptional orientation. Deletion of exon 7 introduces a frameshift. In case of alternative splicing from exon 6 to exon 8, this frameshift would change the last codon of exon 6 to a stop codon, leading to premature termination of the protein. Finally, the modified subcloned 6-kb *BglII* fragment was reinserted into the pGEM5 genomic construct.

Electroporation and selection for recombinant ES cells. 129/OLA-derived E14 embryonic stem (ES) cells were cultured as described elsewhere (25) except that ES cells were cultured on irradiated mouse embryo fibroblast feeder cells. For electroporation, 4×10^7 cells were mixed with 100 μ g of *NotI*-linearized targeting DNA in 600 μ l of phosphate-buffered saline. Electroporation was done in a 0.4-cm cuvette using a Bio-Rad gene pulser (model 1652078) at 3 μ F and 0.8 kV per 0.4 cm. The cells were then seeded on 10-cm-diameter tissue culture dishes without feeder cells. After 1 day, selection was started with hygromycin B (150 mg/ml; Calbiochem). After selection, resistant clones were picked and seeded onto feeder cells.

Southern analysis of ES cells and generation of chimeric mice. Out of 87 hygromycin-resistant clones, 11 were correctly targeted, as confirmed by Southern analysis with a 3' *Oct1* probe (Fig. 1). Hybridization of *EcoRV*-digested genomic DNA with the 3' probe resulted in a wild-type band of 7.8 kb and a mutated band of 5.8 kb. Hybridization of *HindII*-digested genomic DNA with a 5' probe resulted in a wild-type band of 9 kb and a mutated band of 7.7 kb. Absence of additional *pgk-hygro* cassettes inserted elsewhere in the genome was

confirmed by hybridization with a *hygro*-specific probe (data not shown). Chimeric mice were generated by microinjection of two independently targeted ES cell clones into blastocysts. Using this approach, two independent *Oct1*^{-/-} mouse lines were established.

Clinical-chemical analysis of plasma. Standard clinical chemistry analyses on plasma were performed on a Hitachi 911 analyzer to determine levels of bilirubin, alkaline phosphatase, aspartate aminotransferase, alanine aminotransferase, lactate dehydrogenase, creatinine, urea, Na⁺, K⁺, Ca²⁺, Cl⁻, phosphate, total protein, and albumin. For analysis, male 99% FVB wild-type and *Oct1*^{-/-} mice were used ($n = 6$).

Histopathological analysis. Histological and anatomical analyses were performed as described previously (25).

RPA. Total RNA was isolated from mouse tissues by use of TRIzol reagent (Life Technologies, Inc. [GIBCO BRL], Rockville, Md.) according to the manufacturer's instructions. RNase protection analysis (RPA) was performed as described previously (22) with 10 μ g of total RNA per sample. A mouse probe for *Oct1* was made by cloning a 609-nucleotide (nt) PCR fragment (positions 83 to 691 relative to the translation start) into the pGEM-T vector (Promega Corp., Madison, Wis.). After linearization with *AvaII*, a 317-nt antisense RNA probe was generated by transcription with SP6 RNA polymerase, yielding a protected probe fragment of 241 nt. A mouse probe for *Oct2* was made by cloning a 1,147-nt PCR fragment (positions 457 to 1603 relative to the translation start) into the pGEM-T vector. After linearization with *EcoRI*, a 246-nt antisense RNA probe was generated by transcription with SP6 RNA polymerase, yielding a protected probe fragment of 197 nt. A mouse probe for *Oct3* was made by cloning a 1-kb PCR fragment into the pGEM-T Easy vector. After linearization with *NcoI*, a 300-nt antisense RNA probe was generated by transcription with SP6 RNA polymerase, yielding a protected probe fragment of 225 nt (positions 1705 to 1929 relative to the translation start). The mouse *Gapdh* probe was described previously (22).

Northern analysis. Northern blotting was performed according to standard procedures with 20 μ g of total RNA per sample. Blots were hybridized with a 609-nt probe for mouse *Oct1* (positions 83 to 691 relative to the translation start).

Western analysis. Crude membrane fractions were prepared as described elsewhere (20). Protein concentrations were determined using the Bradford protein assay (Bio-Rad Laboratories, Munich, Germany). Proteins were subjected to sodium dodecyl sulfate-polyacrylamide gel electrophoresis and transferred to nitrocellulose (Hybond ECL; Amersham Pharmacia Biotech). The filters were blocked for 1 h at room temperature with TBST (100 mM Tris [pH 7.6], 150 mM NaCl, 0.1% [wt/vol] Tween 20) with 5% skim milk powder. Incubation with an affinity-purified polyclonal antibody (16) against rat *Oct1* (ab1; dilution of 1:5,000) or with an anti-rat cytochrome P450 3A1 (Cyp3A1) monoclonal antibody (dilution 1:1,000) was performed at 4°C overnight (in TBST containing 5% skim milk powder). Antibodies were detected by incubating the blot with horseradish peroxidase-conjugated donkey anti-rabbit (for *Oct1* detection) or goat anti-mouse (for Cyp3A1 detection) IgG for 1 h at room temperature in TBST containing 5% skim milk powder. Antibody binding was visualized with the ECL Western blotting detection system (Amersham Pharmacia Biotech).

Pharmacokinetic experiments. For intravenous (i.v.) drug administration, 5 μ l of drug solution per g of body weight was injected into the tail veins of mice lightly anesthetized with methoxyflurane. Animals were sacrificed at indicated time points by axillary bleeding after anesthesia with methoxyflurane. Gallbladder cannulation experiments were performed as described elsewhere (11), with minor adjustments. For anesthesia, a combination of ketamine (100 mg/kg) and xylazine (6.7 mg/kg) was injected intraperitoneally in a volume of 2.33 μ l per g of body weight. For gallbladder cannulation, after opening of the abdominal cavity and distal ligation of the common bile duct, a polythene catheter (Portex Limited, Hythe, United Kingdom), with an inner diameter of 0.28 mm, was inserted into the incised gallbladder. The catheter was fixed to the gallbladder with an additional ligation. Bile was collected for 60 min after i.v. injection of radiolabeled drug into the tail vein. At the end of the experiment, blood was collected by axillary bleeding. Urine was collected from the bladder, and organs and tissues were removed and homogenized in a 4% (wt/vol) bovine serum albumin solution. Where applicable, intestinal content was separated from intestinal tissue before homogenization. Levels of radioactivity in homogenates were determined as described elsewhere (15).

Statistical analysis. All values are given as means \pm standard deviations (SD). The two-tailed unpaired Student *t* test was used to assess the significance of difference between two sets of data. Differences were considered to be statistically significant when P was <0.05 .

RESULTS

Targeted disruption of *Oct1* and phenotypic analysis. The mouse *Oct1* gene was disrupted by replacing exon 7 with an inverted *pgk-hygro* cassette via homologous recombination in ES cells (Fig. 1). Exon 7 corresponds to the putative TMD7 to -9 in the protein. Correct targeting of the *Oct1* allele in ES cell clones was determined by Southern analysis (data not shown). Using standard blastocyst injection techniques, mice heterozygous and homozygous for the *Oct1* disruption were generated from two independent ES clones. Analysis of a few litters from heterozygous crosses showed that distribution of the three genotypes is according to Mendelian inheritance ($16^{+/+}$, $28^{+/-}$, $14^{-/-}$), indicating that there is no reduced embryonal viability. *Oct1*^{-/-} mice are healthy and fertile. No differences were found in the chemical composition of plasma, and histological analysis of *Oct1*^{-/-} males and females, with an emphasis on liver, kidney, and intestine, revealed no morphological abnormalities. The *Oct1*^{-/-} mice live as long as their wild-type littermates, and no indications have been found for abnormal causes of death.

***Oct1* mRNA and protein analysis.** In the *Oct1*^{-/-} mice, the promoter and exons 1 to 6 of the *Oct1* gene are still intact, potentially allowing transcription and translation of a truncated mRNA upstream of the disruption. Alternative splicing from exon 6 to exon 8 would result in a frameshift, leading to premature termination of the protein. By Northern analysis we could not detect either full-length or truncated *Oct1* mRNA in the liver or kidney of *Oct1*^{-/-} mice, whereas it was readily detectable in wild-type mice (results not shown). To further investigate possible residual transcription of a truncated mRNA, we used RPA, which is more sensitive than Northern analysis, with an RPA probe that recognizes a sequence upstream of the disruption (corresponding to nt 447 to 691 relative to the translation start). An extremely low level of RNA was detected in liver of *Oct1*^{-/-} mice (Fig. 2a), suggesting the presence of a truncated transcript that is far less transcribed or less stable than the full-length mRNA. Translation of this low-abundance truncated mRNA might generate a truncated Oct1 protein, lacking TMD7 to -12, which is unlikely to be functional, stable or properly routed to the plasma membrane. Western analysis, using a polyclonal antibody (16) recognizing the C-terminal part of rat and mouse Oct1, demonstrated that Oct1 protein is undetectable in liver and kidney of *Oct1*^{-/-} mice (Fig. 2b).

We also investigated whether in *Oct1*^{-/-} mice, *Oct2* and *Oct3* are upregulated to compensate for the loss of *Oct1*. With RPA, no differences in expression of *Oct2* and *Oct3* mRNA in the brain, liver, kidney, small intestine, and spleen were observed between *Oct1*^{-/-} and wild-type mice (Fig. 2c). This indicates that the loss of *Oct1* is not compensated for by up-regulation of either *Oct2* or *Oct3* at the mRNA level.

Distribution of [¹⁴C]TEA in *Oct1*^{-/-} and wild-type mice. We first investigated the pharmacologic role of Oct1 by comparing the distribution characteristics of the model substrate TEA in *Oct1*^{-/-} and wild-type mice. TEA is not substantially metabolized in mice, and so radioactivity values give a good representation of unchanged TEA levels (27). Mice received i.v. [¹⁴C]TEA (0.2 mg/kg); after 20 min, levels of radioactivity were measured in plasma, organs, and feces (Table 1). The

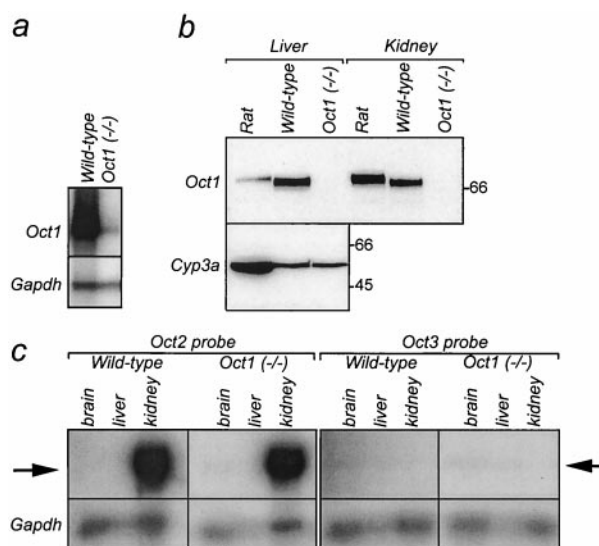


FIG. 2. *Oct1* mRNA and protein analysis. (A) Expression of *Oct1* RNA in livers of wild-type and *Oct1*^{-/-} mice. RPA was performed with 10 μ g of total RNA per sample. *Oct1*- and *Gapdh*-protected RNA fragments originate from the same gel, and their positions are indicated. Note that the specific activity of the *Gapdh* probe was 100-fold lower than that of the *Oct1* probe. (B) Immunodetection of Oct1 in livers and kidneys of wild-type and *Oct1*^{-/-} mice. A polyclonal antibody raised against rat Oct1 (which cross-reacts with mouse Oct1) was used on crude membrane fractions of liver (20 μ g per lane) and kidney (10 μ g per lane). The same blot was incubated with a monoclonal antibody raised against rat cytochrome P450 3a (Cyp3a; expressed only in the liver), used as a protein loading control. Molecular weight marker bands are indicated in kilodaltons. (C) RPA of *Oct2* and *Oct3* RNA in brains, livers, and kidneys of wild-type and *Oct1*^{-/-} mice. Experimental details are as described for panel A. Arrows indicate protected fragments of *Oct2* (left) and *Oct3* (right).

accumulation of [¹⁴C]TEA in the liver was reduced more than sixfold in *Oct1*^{-/-} mice and was $2.8\% \pm 0.7\%$ of the administered dose, compared to $18.1\% \pm 3.3\%$ in wild-type mice. Similarly, levels of excretion of TEA into the lumen of the small intestine, cecum, and colon were all decreased 6- to 10-fold in *Oct1*^{-/-} mice. The contribution of intestinal excretion to the total elimination of TEA, however, was small even in wild-type mice. No significant differences in levels of TEA were found in the brain and spleen, which do not express *Oct1*. Plasma levels of TEA varied considerably but were not significantly different between *Oct1*^{-/-} mice and wild-type mice.

The main route for TEA excretion was via the kidney. The amount of [¹⁴C]TEA found in urine was 1.5-fold higher in *Oct1*^{-/-} mice and was $70.3\% \pm 12.4\%$ of the administered dose, compared to $45.7\% \pm 3.4\%$ in wild-type mice. It should be noted that since these mice were not anesthetized during the experiment, the percentage of TEA recovered from urine might not represent the total amount of TEA excreted via urine, due to urination. Similar effects on TEA distribution and excretion were found in *Oct1*^{-/-} mice derived from an independently targeted ES clone (results not shown).

Excretion of [¹⁴C]TEA in *Oct1*^{-/-} and wild-type mice. Excretion of TEA was more extensively analyzed in fully anesthetized mice with a cannulated gallbladder, allowing accurate measurements of biliary, direct intestinal, and urinary excretion. In these mice, after i.v. administration of [¹⁴C]TEA (0.2

TABLE 1. Levels of radioactivity in female wild-type and *Oct1*^{-/-} mice at 20 min after i.v. injection of [¹⁴C]TEA (0.2 mg/kg)^a

Tissue	Mean ¹⁴ C concn (ng-eq g ⁻¹ or ml ⁻¹) ± SD (n = 4)		Ratio, <i>Oct1</i> ^{-/-} /wt	Mean excretion (%) ± SD (n = 4) ^c		Ratio, <i>Oct1</i> ^{-/-} /wt
	wt	<i>Oct1</i> ^{-/-}		wt	<i>Oct1</i> ^{-/-}	
Plasma	77 ± 60	41 ± 35	0.53			
Brain	2.3 ± 1.5	2.9 ± 2.8	1.24			
Spleen	42 ± 6	42 ± 12	1.02			
Kidney	418 ± 63	584 ± 483	1.40			
Liver	892 ± 283 (18.1 ± 3.3 ^b)	100 ± 33** (2.8 ± 0.7**)	0.11 (0.15)			
Small intestine				2.41 ± 1.00	0.21 ± 0.09**	0.09
Cecum				0.30 ± 0.20	0.05 ± 0.04*	0.16
Colon				0.10 ± 0.06	0.01 ± 0.01*	0.13
Urine				45.7 ± 3.4	70.3 ± 12.4**	1.54

^a wt, wild type; *, *P* < 0.05; **, *P* < 0.01.^b Mean percentage of administered dose ± SD (n = 4).^c Total TEA found in the contents of small intestine, cecum, and colon. Urine was collected from the bladder.

mg/kg), bile was collected every 10 min for 1 h and organs, feces, and urine were collected after 1 h (Table 2). The difference in accumulation of [¹⁴C]TEA in the liver was about four-fold and was 5.8% ± 1.0% of the administered dose in *Oct1*^{-/-} mice, compared to 25.3% ± 0.8% in wild-type mice. In the previous 20-min distribution experiment, the more than 10-fold-diminished excretion into the small intestine could have resulted from both decreased biliary and direct intestinal excretion in the *Oct1*^{-/-} mice. In the gallbladder cannulation experiment, we separately measured direct intestinal and biliary excretion. Over a 1-h period, direct small intestinal excretion was decreased twofold and was 0.67% ± 0.09% in *Oct1*^{-/-} mice, compared to 1.31% ± 0.19% in wild-type mice. Levels of [¹⁴C]TEA in cecum and colon contents were about the same in *Oct1*^{-/-} and wild-type mice.

Whereas the bile flow was not different between wild-type and *Oct1*^{-/-} mice (data not shown), the amount of [¹⁴C]TEA excreted in bile over 1 h was 2.5-fold lower in *Oct1*^{-/-} mice, probably reflecting the difference in liver accumulation of TEA between the two genotypes (Fig. 3). The total percentage of [¹⁴C]TEA excreted via bile in both genotypes, however, was less than 1% of the administered dose, indicating that like intestinal excretion, biliary excretion does not contribute greatly to the elimination of TEA from the body. Thus, despite

the efficient uptake of TEA by Oct1, the liver seems to lack efficient mechanisms to excrete TEA into the bile. Alternatively, liver cells may sequester TEA intracellularly (30). Cumulative excretion of [¹⁴C]TEA in urine was, as in the 20-min distribution experiment, increased 1.5-fold in the *Oct1*^{-/-} mice and represented 80% ± 15.6% of the administered dose, compared to 53.3% ± 16.8% in wild-type mice.

Distribution of other organic cations in *Oct1*^{-/-} and wild-type mice. The effect of absence of Oct1 on pharmacokinetics was also investigated for several other organic cations of toxicological, clinical, and physiological interest (Table 3). We compared the distribution characteristics of wild-type and *Oct1*^{-/-} mice at 30 min after i.v. administration of [³H]MPP⁺, [¹²⁵I]MIBG, [³H]cimetidine, and [¹⁴C]choline, each at 1 mg/kg. The neurotoxin MPP⁺ has previously been shown to be transported in vitro by rat Oct1 (7, 14). The drug MIBG is used in diagnosis and treatment of tumors of neuroadrenergic origin, such as neuroblastoma (28). MIBG is a metabolically stable analogue of norepinephrine, a known Oct1 substrate (1), suggesting that it might also be transported by Oct1. The hepatic uptake of [³H]MPP⁺ and [¹²⁵I]MIBG in *Oct1*^{-/-} mice was reduced about 60 and 75%, respectively. At the same time, no significant differences were found in plasma, spleen, or small intestinal excretion of these compounds (Table 3). Both com-

TABLE 2. Levels of radioactivity in female wild-type and *Oct1*^{-/-} mice with a cannulated gallbladder at 60 min after i.v. injection of [¹⁴C]TEA (0.2 mg/kg)^a

Tissue	Mean ¹⁴ C concn (ng-eq g ⁻¹ or ml ⁻¹) ± SD (n = 4)		Ratio, <i>Oct1</i> ^{-/-} /wt	Mean excretion (%) ± SD (n = 4) ^c		Ratio, <i>Oct1</i> ^{-/-} /wt
	wt	<i>Oct1</i> ^{-/-}		wt	<i>Oct1</i> ^{-/-}	
Plasma	23.8 ± 4.9	17.1 ± 3.0*	0.72			
Brain	1.6 ± 0.3	1.9 ± 0.4	1.22			
Spleen	35 ± 5	42 ± 2*	1.21			
Kidney	441 ± 152	236 ± 20*	0.53			
Liver	1,225 ± 26 (25.3 ± 0.8 ^b)	283 ± 44** (5.8 ± 1.0**)	0.23 (0.23)			
Bile				0.35 ± 0.09	0.14 ± 0.01*	0.41
Small intestine				1.31 ± 0.19	0.67 ± 0.09**	0.51
Cecum				0.12 ± 0.02	0.09 ± 0.04*	0.72
Colon				0.03 ± 0.01	0.04 ± 0.01	1.23
Urine				53.3 ± 16.8	80.0 ± 15.6*	1.50

^a wt, wild type; *, *P* < 0.05; **, *P* < 0.01.^b Mean percentage of administered dose ± SD (n = 4).^c Total TEA found in the contents of small intestine, cecum, and colon. Urine was collected from the bladder.

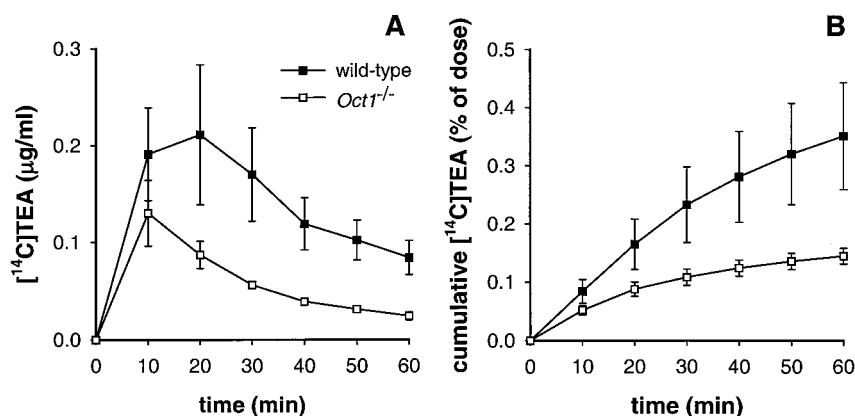


FIG. 3. Biliary excretion of TEA in wild-type and *Oct1*^{-/-} mice with a cannulated gallbladder. (A) Concentration of [¹⁴C]TEA in collected bile fractions. (B) Cumulative excretion of [¹⁴C]TEA in bile. Bile was collected at 10-min intervals for 1 h after i.v. administration of [¹⁴C]TEA (0.2 mg/kg) to wild-type and *Oct1*^{-/-} mice. Results are means \pm SD ($n = 4$).

pounds were primarily excreted in the urine (data not shown), and both are, at least in humans, metabolized to only a minor degree, and so total radioactivity will likely give a good representation of unchanged drug levels (9, 31).

The antihistamine cimetidine has been used as a model compound in organic cation transport studies. In humans, cimetidine is excreted primarily in the urine without being metabolized (17). In vitro studies with transfected cells suggest that cimetidine can inhibit Oct1 but is not transported by it (35). Choline is an essential nutrient, being required, for example, for the synthesis of phosphatidylcholine in the liver and acetylcholine in neuronal cells. In vitro transport of choline has been demonstrated in rat *Oct1*-microinjected *Xenopus* oocytes (2) and in murine *Oct1*-transfected BALB/3T3 cells (24). For

both [³H]cimetidine and [¹⁴C]choline, we observed no significant differences in the distribution to liver or other organs between wild-type and *Oct1*^{-/-} mice (Table 3).

DISCUSSION

Our results show that Oct1 in itself is not essential for normal health and fertility of mice, but that it has an important role in the pharmacokinetics of several organic cationic drugs and toxins. In rodents, *Oct1* is expressed in the three major excretory organs, i.e., liver, kidney, and small intestine, and absence of this protein might thus result in decreased excretion of substrates via these organs. The pharmacologic role of Oct1 is clearly illustrated by comparing the pharmacokinetics of the

TABLE 3. Levels of radioactivity in wild-type and *Oct1*^{-/-} mice 30 min after i.v. injection of [³H]cimetidine, [¹²⁵I]MIBG, [³H]MPP⁺, or [¹⁴C]choline (1 mg/kg)^a

Drug	Tissue	Mean [³ H], [¹⁴ C], or [¹²⁵ I] concn (ng-eq g ⁻¹ or ml ⁻¹) \pm SD		Ratio, <i>Oct1</i> ^{-/-} /wt
		wt	<i>Oct1</i> ^{-/-}	
[³ H]MPP ⁺	Liver	1,989 \pm 752 (7.9 \pm 3.1 ^b)	757 \pm 218* (3.1 \pm 0.7*)	0.38 (0.39)
	Sm. int.	5.7 \pm 2.0 ^c	3.0 \pm 1.1 ^c	0.52
	Kidney	2,292 \pm 1,341	2,219 \pm 1,992	1.03
	Spleen	2,736 \pm 537	3,210 \pm 939	1.17
	Plasma	94.9 \pm 18.7	126 \pm 40.5	1.32
[¹²⁵ I]MIBG	Liver	2,600 \pm 680 (10.4 \pm 1.49)	607 \pm 135** (2.80 \pm 0.65**)	0.23 (0.27)
	Sm. int.	2.09 \pm 0.94 ^c	0.97 \pm 0.33 ^c	0.46
	Kidney	1,333 \pm 236	1,145 \pm 236	0.86
	Spleen	1,065 \pm 136	1,175 \pm 223	1.10
	Plasma	229 \pm 54.7	214 \pm 43.7	0.93
[³ H]cimetidine	Liver	655 \pm 10.7 (2.87 \pm 0.08)	528 \pm 85.4 (2.32 \pm 0.50)	0.81 (0.81)
	Sm. int.	2.03 \pm 0.91 ^c	3.11 \pm 0.36 ^c	1.53
	Kidney	1,584 \pm 412	1,194 \pm 473	0.75
	Spleen	202 \pm 16.0	209 \pm 26.8	1.03
	Plasma	333 \pm 39.7	317 \pm 88.1	0.95
[¹⁴ C]choline	Liver	13,248 \pm 4,056 (58.7 \pm 16.9)	14,000 \pm 1,445 (69.3 \pm 7.8)	1.06 (1.18)
	Sm. int.	4.8 \pm 2.1 ^c	6.5 \pm 4.0 ^c	1.35
	Kidney	11,777 \pm 1,531	10,066 \pm 251	0.85
	Spleen	3,804 \pm 1,166	3,737 \pm 968	0.98
	Plasma	619 \pm 80.0	540 \pm 50.4	0.87

^a wt, wild type; Sm. int., small intestine; *, $P < 0.05$; **, $P < 0.01$. Experiments with cimetidine and MIBG were performed in females ($n = 3$); experiments with MPP⁺ and choline were performed in males ($n = 4$).

^b Mean percentage of administered dose \pm SD.

^c Mean percentage of dose in small intestinal contents.

model substrate TEA in wild-type and *Oct1*^{-/-} mice. The accumulation of i.v.-administered TEA in liver of *Oct1*^{-/-} mice was dramatically reduced (to 15 and 23% of levels in wild-type mice after 20 and 60 min, respectively), indicating that for TEA, Oct1 is the main uptake system in the liver. In addition, direct small intestinal excretion in *Oct1*^{-/-} mice was reduced to about 50% of wild-type levels, showing that Oct1 also mediates basolateral uptake of TEA into enterocytes.

The main excretory route for TEA is via the kidney, and about 53% was excreted renally after 60 min in wild-type mice. In *Oct1*^{-/-} mice, the amount of TEA in urine was significantly increased, to about 80% of the dose. These findings seem to contradict a direct role for Oct1 in renal secretion, but they can be explained by the altered pharmacokinetics due to the absence of Oct1 in the liver. In wild-type mice, about 20% of the total TEA administered rapidly accumulates in the liver, compared to only about 3% in *Oct1*^{-/-} mice. Shortly after i.v. injection, this may lead to higher drug availability in plasma of *Oct1*^{-/-} mice, resulting in rapid excretion by the kidney. Thus, we think that the increase in renal excretion of TEA can be explained as a secondary effect of the absence of Oct1 in the liver. The exact role of Oct1 in the kidney is still to be established, but from these data, Oct1 alone does not seem to play a crucial role in the renal elimination of TEA. Renal clearance of compounds is dependent on their rate of filtration, secretion, and reabsorption. For TEA, it has been shown that renal clearance is mediated mainly by secretion (19). Besides Oct1, Oct2 is also highly expressed in kidney. Since these two transporters have overlapping substrate specificities and are both localized at the basolateral membrane of proximal tubule cells in the kidney, loss of one might well be compensated for by the other. Therefore, to further investigate the role of the polyspecific cation transporters in kidney, we are generating *Oct2* knockout mice as well as *Oct1/2* double-knockout mice.

We further found that the neurotoxin MPP⁺ and the norepinephrine analogue MIBG are efficiently transported in vivo by Oct1, as indicated by the ~4-fold-reduced liver accumulation in *Oct1*^{-/-} mice. No significant differences were found for these compounds in intestinal excretion, which may be explained by the presence of alternative uptake transporters for these compounds in intestine. Clinically, [¹³¹I]MIBG is used in detection and treatment of tumors of neuroadrenergic origin, such as neuroblastoma and pheochromocytoma (28). MIBG is selectively taken up by these tumors due to expression of the norepinephrine transporter, which is part of the neuronal uptake system referred to as uptake₁ (5). In addition to transport by the norepinephrine transporter, it has been suggested that MIBG is also transported by the extraneuronal uptake₂ system as well as by another, yet unidentified, sodium- and energy-independent transport system (3, 10). Our findings suggest that this latter sodium- and energy-independent transport of MIBG is mediated, at least in part, by Oct1.

We did not find a significant involvement of Oct1 in the distribution of [³H]cimetidine and [¹⁴C]choline. For cimetidine, this result is in line with studies with *Oct1*-transfected cells that suggest that cimetidine can inhibit Oct1 but is not transported by it (35). In previous in vitro studies, transport of choline has been demonstrated in rat *Oct1*-microinjected *Xenopus* oocytes (2) and in murine *Oct1*-transfected BALB/3T3 cells (24). Here, we found that 30 min after i.v. administration

of [¹⁴C]choline, about 60 to 70% of radioactivity was present in livers of both wild-type and *Oct1*^{-/-} mice, suggesting the presence of efficient uptake systems for choline other than Oct1 in the liver. This redundancy in choline uptake may partly explain why we did not observe an effect of the absence of Oct1 on its pharmacokinetics. Alternatively, rapid metabolism of [¹⁴C]choline into labeled compounds that are not transported by Oct1, but still accumulate efficiently in liver, might also mask a possible effect. The homeostasis of endogenous organic cations, such as choline and catecholamines, is strictly regulated at the level of production, transport, and metabolism, and absence of one of these functions is likely to be compensated for. Oct2 and, to a lesser extent, Oct3 have overlapping substrate specificities with Oct1 and therefore may be partly redundant in tissues where they are present together with Oct1. However, we did not find increased levels of *Oct2* or *Oct3* mRNA in *Oct1*^{-/-} mice, indicating that loss of *Oct1* is not compensated for by upregulation of one of these genes.

In conclusion, we have generated an *Oct1* knockout mouse line which exhibits greatly reduced hepatic uptake and direct intestinal excretion of substrate organic cations. Since Oct1 is a polyspecific transporter, it might be of importance in the pharmacokinetics of many endogenous compounds as well as toxins and clinically used drugs. Also, it will be of great interest to investigate the physiological and/or pharmacological complementarity between Oct1 and various other basolateral and apical drug transporters, by breeding with suitable knockout strains lacking these transporters. Knowledge of the mechanisms that contribute to the transport and elimination of drugs will possibly allow prediction and rational manipulation of their pharmacokinetics and prevention of possible side effects.

ACKNOWLEDGMENTS

We thank our colleagues for critical reading of the manuscript, S. Van Eijl and A. Otten for excellent technical assistance, and M. Van der Valk for histological analysis.

This work was supported in part by grant NKI 97-1434 (to A. H. Schinkel) from the Dutch Cancer Society.

REFERENCES

- Breider, T., F. Spitzenberger, D. Gründemann, and E. Schömig. 1998. Catecholamine transport by the organic cation transporter type 1 (OCT1). *Br. J. Pharmacol.* **125**:218–224.
- Busch, A. E., S. Quester, J. C. Ulzheimer, S. Waldegger, V. Gorboulev, P. Arndt, F. Lang, and H. Koepsell. 1996. Electrogenic properties and substrate specificity of the polyspecific rat cation transporter rOCT1. *J. Biol. Chem.* **271**:32599–32604.
- Degrado, T. R., M. R. Zalutsky, and G. Vaidyanathan. 1995. Uptake mechanisms of meta-[¹²⁵I]iodobenzylguanidine in isolated rat heart. *Nucl. Med. Biol.* **22**:1–12.
- Dresser, M. J., L. Zhang, and K. M. Giacomini. 1999. Molecular and functional characteristics of cloned human organic cation transporters. *Pharm. Biotechnol.* **12**:441–469.
- Glowniak, J. V., J. E. Kilty, S. G. Amara, B. J. Hoffman, and F. E. Turner. 1993. Evaluation of metaiodobenzylguanidine uptake by the norepinephrine, dopamine and serotonin transporters. *J. Nucl. Med.* **34**:1140–1146.
- Gorboulev, V., J. C. Ulzheimer, A. Akhoundova, I. Ulzheimer-Teuber, U. Karbach, S. Quester, C. Baumann, F. Lang, A. E. Busch, and H. Koepsell. 1997. Cloning and characterization of two human polyspecific organic cation transporters. *DNA Cell Biol.* **16**:871–881.
- Gründemann, D., V. Gorboulev, S. Gambaryan, M. Veyhl, and H. Koepsell. 1994. Drug excretion mediated by a new prototype of polyspecific transporter. *Nature* **372**:549–552.
- Gründemann, D., S. Köster, N. Kiefer, T. Breider, M. Engelhardt, F. Spitzenberger, N. Obermüller, and E. Schömig. 1998. Transport of monoamine transmitters by the organic cation transporter type 2, OCT2. *J. Biol. Chem.* **273**:30915–30920.
- Irwin, I., L. E. DeLanney, D. Di Monte, and J. W. Langston. 1989. The

- biodisposition of MPP⁺ in mouse brain. *Neurosci. Lett.* **101**:83–88.
10. **Jaques, S., M. C. Tobes, J. C. Sisson, J. A. Baker, and D. M. Wieland.** 1984. Comparison of the sodium dependency of uptake of meta-iodobenzylguanidine and norepinephrine into cultured bovine adrenomedullary cells. *Mol. Pharmacol.* **26**:539–546.
 11. **Jonker, J. W., E. Wagenaar, L. van Deemter, R. Gottschlich, H. M. Bender, J. Dasenbrock, and A. H. Schinkel.** 1999. Role of blood-brain barrier P-glycoprotein in limiting brain accumulation and sedative side-effects of aspidolone, a peripherally acting analgesic drug. *Br. J. Pharmacol.* **127**:43–50.
 12. **Karbach, U., J. Kricke, F. Meyer-Wentrup, V. Gorboulev, C. Volk, D. Löffing-Cueni, B. Kaissling, S. Bachmann, and H. Koepsell.** 2000. Localization of organic cation transporters OCT1 and OCT2 in rat kidney. *Am. J. Physiol. Renal Physiol.* **279**:F679–F687.
 13. **Koepsell, H.** 1998. Organic cation transporters in intestine, kidney, liver, and brain. *Annu. Rev. Physiol.* **60**:243–266.
 14. **Martel, F., T. Vetter, H. Russ, D. Gründemann, I. Azevedo, H. Koepsell, and E. Schömig.** 1996. Transport of small organic cations in the rat liver. The role of the organic cation transporter OCT1. *Naunyn-Schmiedeberg's Arch. Pharmacol.* **354**:320–326.
 15. **Mayer, U., E. Wagenaar, J. H. Beijnen, J. W. Smit, D. K. F. Meijer, J. van Asperen, P. Borst, and A. H. Schinkel.** 1996. Substantial excretion of digoxin via the intestinal mucosa and prevention of long-term digoxin accumulation in the brain by the mdrla P-glycoprotein. *Br. J. Pharmacol.* **119**:1038–1044.
 16. **Meyer-Wentrup, F., U. Karbach, V. Gorboulev, P. Arndt, and H. Koepsell.** 1998. Membrane localization of the electrogenic cation transporter rOCT1 in rat liver. *Biochem. Biophys. Res. Commun.* **248**:673–678.
 17. **Mitchell, S. C., J. R. Idle, and R. L. Smith.** 1982. The metabolism of [¹⁴C]cimetidine in man. *Xenobiotica* **12**:283–292.
 18. **Nagel, G., C. Volk, T. Friedrich, J. C. Ulzheimer, E. Bamberg, and H. Koepsell.** 1997. A reevaluation of substrate specificity of the rat cation transporter rOCT1. *J. Biol. Chem.* **272**:31953–31956.
 19. **Nelson, J. A., J. F. Kuttesch, and B. H. Herbert.** 1983. Renal secretion of nucleosides and their analogs in mice. *Biochem. Pharmacol.* **32**:2323–2327.
 20. **Ogihara, H., H. Saito, B. Shin, T. Terada, S. Takenoshita, Y. Nagamachi, K. Inui, and K. Takata.** 1996. Immuno-localization of H⁺/peptide cotransporter in rat digestive tract. *Biochem. Biophys. Res. Commun.* **220**:848–852.
 21. **Okuda, M., H. Saito, Y. Urakami, M. Takano, and K. Inui.** 1996. cDNA cloning and functional expression of a novel rat kidney organic cation transporter, OCT2. *Biochem. Biophys. Res. Commun.* **224**:500–507.
 22. **Schinkel, A. H., J. J. M. Smit, O. van Tellingen, J. H. Beijnen, E. Wagenaar, L. van Deemter, C. A. A. M. Mol, M. A. van der Valk, E. C. Robanus-Maandag, H. P. Te Riele, A. J. M. Berns, and P. Borst.** 1994. Disruption of the mouse mdrla P-glycoprotein gene leads to a deficiency in the blood-brain barrier and to increased sensitivity to drugs. *Cell* **77**:491–502.
 23. **Schweifer, N., and D. P. Barlow.** 1996. The Lx1 gene maps to mouse chromosome 17 and codes for a protein that is homologous to glucose and polyspecific transmembrane transporters. *Mamm. Genome* **7**:735–740.
 24. **Sinclair, C. J., K. D. Chi, V. Subramanian, K. L. Ward, and R. M. Green.** 2000. Functional expression of a high affinity mammalian hepatic choline/organic cation transporter. *J. Lipid Res.* **41**:1841–1848.
 25. **Smit, J. J. M., A. H. Schinkel, R. P. J. Oude Elferink, A. K. Groen, E. Wagenaar, L. van Deemter, C. A. A. M. Mol, R. Ottenhof, N. M. T. van der Lugt, M. A. van Roon, M. A. van der Valk, G. J. A. Offerhaus, A. J. M. Berns, and P. Borst.** 1993. Homozygous disruption of the murine mdrla P-glycoprotein gene leads to a complete absence of phospholipid from bile and to liver disease. *Cell* **75**:451–462.
 26. **Tamai, I., H. Yabuuchi, J. Nezu, Y. Sai, A. Oku, M. Shimane, and A. Tsuji.** 1997. Cloning and characterization of a novel human pH-dependent organic cation transporter, OCTN1. *FEBS Lett.* **419**:107–111.
 27. **Taylor, P.** 1992. Agents acting at the neuromuscular junction and autonomic ganglia, p. 166–185. *In* A. Goodman Gilman, T. W. Rall, A. S. Nies, and P. Taylor (ed.), *The pharmacological basis of therapeutics*. McGraw-Hill, New York, N.Y.
 28. **Trocone, L., and V. Rufini.** 1997. ¹³¹I-MIBG therapy of neural crest tumours. *Anticancer Res.* **17**:1823–1831. (Review.)
 29. **Urakami, Y., M. Okuda, S. Masuda, H. Saito, and K. Inui.** 1998. Functional characteristics and membrane localization of rat multispecific organic cation transporters, OCT1 and OCT2, mediating tubular secretion of cationic drugs. *J. Pharmacol. Exp. Ther.* **287**:800–805.
 30. **Van Dyke, R. W., E. D. Faber, and D. K. F. Meijer.** 1992. Sequestration of organic cations by acidified hepatic endocytic vesicles and implications for biliary excretion. *J. Pharmacol. Exp. Ther.* **261**:1–11.
 31. **Wafelman, A. R., Y. L. Nortier, H. Rosing, H. J. Maessen, B. G. Taal, C. A. Hoefnagel, R. A. Maes, and J. H. Beijnen.** 1995. Renal excretion of meta-iodobenzylguanidine after therapeutic doses in cancer patients and its relation to dose and creatinine clearance. *Nucl. Med. Commun.* **16**:767–772.
 32. **Wieland, D. M., J. L. Wu, L. E. Brown, T. J. Mangner, D. P. Swanson, and W. H. Beierwaltes.** 1980. Radiolabeled adrenergic neuron-blocking agents: adrenomedullary imaging with [¹³¹I]-iodobenzylguanidine. *J. Nucl. Med.* **21**:349–353.
 33. **Wu, X., R. Kekuda, W. Huang, Y. Fei, F. H. Leibach, J. Chen, S. J. Conway, and V. Ganapathy.** 1998. Identity of the organic cation transporter OCT3 as the extraneuronal monoamine transporter (uptake2) and evidence for the expression of the transporter in the brain. *J. Biol. Chem.* **273**:32776–32786.
 34. **Wu, X., P. D. Prasad, F. H. Leibach, and V. Ganapathy.** 1998. cDNA sequence, transport function, and genomic organization of human OCTN2, a new member of the organic cation transporter family. *Biochem. Biophys. Res. Commun.* **246**:589–595.
 35. **Zhang, L., M. E. Schaner, and K. M. Giacomini.** 1998. Functional characterization of an organic cation transporter (hOCT1) in a transiently transfected human cell line (HeLa) *J. Pharmacol. Exp. Ther.* **286**:354–361.